DOI: 10.36108/ujees/3202.50.0151



UNIOSUN Journal of Engineering and Environmental Sciences. Vol. 5 No. 1. March. 2023

An Analysis of Buoyancy-Driven Heat Behaviour and Flow Pattern of a Water-Copper Nanofluid in a Cylindrical Conduit

Itabiyi, O.E., Sangotayo, E.O. and Ogidiga, J.O.

Abstract: The flow of fluids and heat characteristics through free convection within an enclosed space has gained substantial study due to the various applications in manufacturing industries. This work examined the influence of buoyancy factors on normal convection in a heated tube filled with Copper (Cu) nanofluid. The method of finite difference was employed to characterize the regulating fluid formulae, and C++ programming language was employed to evaluate the Navier Stoke and continuity fields. This study examined Cu nanoparticles with particle sizes ranging from 1% to 10% and buoyancy values between 2.6 x 10³ and 2.8 x 10³ N. Cu nanofluid was used as the working fluid and the findings are presented as temperature gradient, Nusselt number, stream function, and vorticity curves. The findings revealed that an increase in the weight proportions of nanoparticles to 0.04 amplifies the buoyancy parameters to the highest value of 2.75 x 10³ N; it yields a substantial enhancement in the heat transport rate by convection. Also, as the buoyancy factor increases, the temperature gradient, vorticity, and stream function of the nanofluid improve, while the local drag coefficient decreases. This study advances the understanding of buoyancy-driven convective flow and heat behavior in the technical design of floating vessels for safety and effectiveness.

Keywords: Nanofluid, Natural Convection, Cylindrical Cavity, Buoyancy parameter, Finite Difference Scheme

I. Introduction

Many theoretical and applied research papers on equipment, cooling electrical military, biomedical, radiators, etc. have focused on natural convection. Nanofluids cool electronic chips, computers, cars, and medical devices due superior thermal characteristics. their Electronic cooling, vapour absorption refrigeration, heat ventilation, nuclear reactor moderation, and air conditioning all take convective buoyancy-induced natural exchange into account [1,2]. Nanofluids are employed as a working fluid to get around

Itabiyi, O.E., Sangotayo, E.O. and Ogidiga, J.O.

(Department of Mechanical Engineering, Ladoke
Akintola University of Technology, Ogbomoso, Nigeria)

Corresponding author: eosangotayo@lautech.edu.ng
Phone Number: +234-8032317426

issues with conventional micro fluids including abrasion, clogging, quick sedimentation, and large pressure loss, In addition to the great thermal efficiency, nanofluids have special thermal properties, such as elevated surface-tovolume proportion and strong conductivities. Nanofluids are considered a successful technique for reducing carbon emissions, reducing the effects of global warming, and, most importantly, ending our reliance on fossil fuels. Nanofluids are therefore frequently used in the heat extraction industry, for example, in the cooling of electrical circuits. Recent studies focused on the use of nanofluids to improve heat transmission and its utility in the cooling industry. [3, 4]

The author [5] looked at how well heat transfer functioned in an enclosed space with nanofluids

and a focused heat source and Nanofluids can improve heat transfer compared to regular fluids, according to the findings of lattice Boltzmann modeling, which has led to the shrinking of a variety of industrial equipment. The capacity proportion of nanoparticles was shown to enhance the mean Nusselt number [6], Nada's simulation of heat transmission and fluid flow produced by buoyant forces in a partially heated container containing nanofluids. examined laminar translational transmission in a vertical annulus with solid cylinders that generated heat within using natural convection and conduction. The findings showed that the range in which the uncertainty associated with heat transfer may be changed by nanoparticle size. The heat transmission and fluid flow of spontaneous convection of an Aluminum-water nanofluid in an enclosed space were studied with partially heated walls and the impacts of nanoparticles are magnified when the Prandtl number is reduced [8]. [9] examined the impact of nanofluids on heat transfer for a range of relevant factors in a trapezoidal enclosure. The findings showed that a steep sloping wall and a significant amount of Cu nanoparticles can significantly speed up heat transmission.

Experimental investigation of Al₂O₃/water-free convection heat transport revealed that nanofluids with weight fractions from 0 to 8% showed enhanced heat transfer for volume fractions between 0.2% and 2% and decreased efficiency for volume concentrations exceeding 2% [10]. The thermophysical characteristics of Al₂O₃ and TiO₂ metallic oxide particles distributed in water were examined and it was revealed that nanofluids exhibited significantly better heat conductivity than regular liquids [11]. [12] studied spontaneous convective heat transfer in a horizontal cylindrical container containing TiO2 nanoparticles dispersed in deionized water, and [13] examined free convective heat transport of titanium dioxide nanoparticle suspensions. [14] investigated

turbulent free convection heat transmission in nanofluid thermal stratification, the results demonstrated that nanofluids in an enclosure significantly affected the effectiveness of heat transfer. [15] found enhancements at lowweight fractions and degradation at high concentrations of nanoparticles in turbulent heat transfer by free convection. [16] examined the free convective transfer of heat at different nanofluid volume concentrations in rectangular duct with partly heated vertical sidewalls. Heat exchange increased by 15% relative to water at 0.1% weight fractions [17]. [18] statistically evaluated free convection heat exchange in a lateral tube containing Al₂O₃water nanofluid at percentages from 1% to 4% by volume and the Nusselt factor enhanced with Rayleigh value. Omer et al. [19] used SiO, nanofluid to model free convection heat transport in a concentric horizontal annulus and the mean Nusselt value increased with the Rayleigh parameter. [20] employed nanoparticles and water as the foundation fluid in a computer investigation to figure out how aspect ratio affects nanofluid heat transfer through un-induced convection and raising the nanoparticle value from 0.01 to 0.2 increases the average Nusselt values by 50.4%. [21] described buoyancy-induced spontaneous convective heat transfer by vibration on the cylindrical surface in a prismatic container filled with transformer oil - TiO2 and the temperature rose axially and fell radially. [22] investigated how Richardson parameters affected heat behaviour and flow pattern in a tube filled with nanoparticles at various weight percentages and Richardson variables greatly affect heat transmission.

The review of the literature found that less study has been done on how the buoyancy factor affects heat transfer by free convection through a cylindrical duct. This study examines the consequence of buoyancy parameters on free convection in an enclosed space with a hot H₂O- Cu nanofluid-filled cylinder channel. Buoyancy is essential in the design of underground concrete foundations and resisting water's buoyant forces prevents the structure from floating or shifting upward.

II. Materials and Methods A. Numerical Model

Figure 1 shows the two-dimensional laminar boundary layer flow of an incompressible Newtonian fluid with viscous fluid on the cylinder's surface. The surface temperature is greater than the free stream temperature and water contains copper nanoparticles. Laminar natural convection heat transport was simulated in a saturated H₂O-Cu nanofluid vertical cylinder. Free circulation and fluid motion relative to the solid surface come from density change-induced buoyancy and the momentum field accounts for buoyancy forces as body forces. These conditions link continuity, momentum, and energy equations. thermophysical properties stated in Table 1 are considered to be constant. [6].

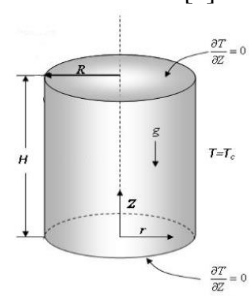


Figure 1: Geometrical configuration, boundary conditions, and coordinate system

B. Governing Equations

The driving mathematical equations were solved assuming fluid incompressibility, laminar flow,

no internal heat inputs, two-dimensional flow, the Boussinesq approximation, and thermal equilibrium between water and nanoparticles. The present model suggests steady, two-dimensional, laminar, incompressible, viscousfree flow, and gravity acts vertically downward, but radiation is ignored. Over the continuum, flow-regulating formulae are mass and momentum conservation formulae [7, 8]:

The continuity formula is expressed in Eq. (1)

$$\frac{\partial \rho}{\partial t} + \frac{1}{r} \frac{\partial (\rho r v_{,})}{\partial r} + \frac{1}{r} \frac{\partial (\rho v_{,})}{\partial \theta} + \frac{\partial (\rho v_{,})}{\partial z} = 0.$$
 (1)

R and Z Navier-Stokes equations are Eq. (2) and Eq. (3).

$$\rho \left(\frac{\partial v_{r}}{\partial t} + v_{r} \frac{\partial v_{r}}{\partial r} + \frac{v_{\theta}}{r} \frac{\partial v_{r}}{\partial \theta} + v_{z} \frac{\partial v_{r}}{\partial z} - \frac{v_{\theta}^{2}}{r} \right) \\
= -\frac{\partial p}{\partial r} + \mu \left[\frac{\partial}{\partial r} \left(\frac{1}{r} \frac{\partial}{\partial r} (rv_{r}) \right) + \frac{1}{r^{2}} \frac{\partial^{2} v_{r}}{\partial \theta^{2}} + \frac{\partial^{2} v_{r}}{\partial z^{2}} - \frac{2}{r} \frac{\partial v_{\theta}}{\partial \theta} \right] + \rho g_{r}$$
(2)

$$\rho \left(\frac{\partial v_{z}}{\partial t} + v_{r} \frac{\partial v_{z}}{\partial r} + \frac{v_{\theta}}{r} \frac{\partial v_{z}}{\partial \theta} + v_{z} \frac{\partial v_{z}}{\partial z} \right) \\
= -\frac{\partial p}{\partial z} + \mu \left[\frac{1}{r} \frac{\partial}{\partial r} \left(r \frac{\partial v_{z}}{\partial r} \right) + \frac{1}{r^{2}} \frac{\partial^{2} v_{z}}{\partial \theta^{2}} + \frac{\partial^{2} v_{z}}{\partial z^{2}} \right] + \rho g_{z}$$
(3)

Equation (4) provides the formula for thermal energy exchange

$$\rho_{sl}(c_{p})_{sl}\left(u\frac{\partial T}{\partial r}+v\frac{\partial T}{\partial z}\right)=k_{sl}\left(\frac{\partial^{2}T}{\partial r^{2}}+v\frac{\partial^{2}T}{\partial z^{2}}\right). \tag{4}$$

The nanofluid heat capacity $(c_p)_{nf}$, density, ρ_{nf} , thermal expansion coefficient, β_{nf} , and thermal diffusivity, α_{nf} are expressed in Eq. (5-11) [9, 10, 11].

Equation (5) provides an approximation of the nanofluid's effective thermal conductivity

$$\frac{k_{nf}}{k_{f}} = \frac{k_{cu} + 2k_{f} - 2\varphi(k_{f} - k_{cu})}{k_{cu} + 2k_{f} + \varphi(k_{f} - k_{cu})}$$
(5)

Tuble 1. Water Ga I tallollara 5 Thermophysical Gharacteristics [6]							
	Density (kgm ⁻³)	Heat Capacity	Thermal	Thermal	Viscosity		
		$(J/kg^{-1}K^{-1})$	Conductivity	expansion (K-1)			
			(Wm ⁻¹ K ⁻¹)				
H ₂ O	997.1	4179	0.613	21x10 ⁻⁵	9.09x10 ⁻⁵		
Cu	8954	383	400	1.67x10 ⁻⁵			

Table 1: Water-Cu Nanofluid's Thermophysical Characteristics [6]

This equation only applies to spherical nanoparticles and does not take into consideration other nanoparticle shapes. This model is suitable for researching nanofluidenhanced heat transfer [7, 10]. The nanofluid's viscosity is given in Eq.(6) [11]:

$$\mu_{nf} = \mu_f \left(1 - \varphi \right)^{-2.5} \tag{6}$$

Equation (7) is the formula for the nanofluid's density [10]

$$\rho_{nf} = (1 - \varphi)\rho_f + \varphi \rho_{cu} \tag{7}$$

Equation (8) expresses the nanofluid's heat capacitance [10, 11]:

$$\left(\rho c_{p}\right)_{nf} = \left(1 - \varphi\right)\left(\rho c_{p}\right)_{f} + \varphi\left(\rho c_{p}\right)_{cu} \tag{8}$$

The nanofluid's thermal expansion coefficient is written in Eq (9) [11]

$$(\rho\beta)_{nf} = (1 - \varphi)(\rho\beta)_{f} + \varphi(\rho\beta)_{cu}$$
(9)

Eq. (10) provides the nanofluid's thermal diffusivity [11]

$$\alpha_{nf} = \frac{k_{nf}}{\left(\rho c_p\right)_{nf}} \tag{10}$$

C. Analytical Techniques and Solution Schemes

Parabolic, elliptic, or hyperbolic Navier-Stokes equations are partial derivative formulae. The vorticity-stream technique was used to eliminate the pressure gradient between the two equations (2) and (3). Using the continuity concept in equation (1), the vortex shedding transport expression is presented in equation (11)

$$\omega = \frac{\partial v}{\partial r} - \frac{\partial u}{\partial z} \tag{11}$$

The dimensional vorticity transmission equation is given in equation (12)

$$u\frac{\partial\omega}{\partial r} + v\frac{\partial\omega}{\partial z} = -\beta g\frac{\partial T}{\partial r} + \upsilon\left(\frac{\partial^2\omega}{\partial r^2} + \frac{\partial^2\omega}{\partial z^2}\right)$$
(12)

Equation (13) utilizes stream function derivatives to define velocity in two-dimensional cylindrical dimensions.

$$u = \frac{\partial \psi}{\partial z}, \quad v = -\frac{\partial \psi}{\partial r} \tag{13}$$

Equation (14) offers the Poisson formula when substituted in Eq.(11)

$$\omega = -\left(\frac{\partial^2 \psi}{\partial r^2} + \frac{\partial^2 \psi}{\partial z^2}\right) \tag{14}$$

The transport equation, energy equation, and operational conditions were translated to a non-dimensional notation for various physical parameters using L, U_W , $(T_{\rm w}$ - $T_{\infty})$, $\psi_W L$, and

 ω_{W}/L respectively for length, velocity, temperature, stream function, and vorticity as shown in Eq.(15), [3].

$$Z = \frac{z}{L}, \quad R = \frac{r}{L}, \quad V = \frac{v}{U_{v}}, \quad U = \frac{u}{U_{v}},$$

$$\theta = \frac{\left(T - T_{v}\right)}{\left(T_{v} - T_{v}\right)}, \quad \Omega = \frac{\omega}{U_{v}/L}, \quad \Psi = \frac{\psi}{U_{v}L}, \tag{15}$$

Eq. (16–19) provides the normalized equations for the R- and Z-velocity components, vortex shedding, stream constituent, and energy transport:

$$U = \frac{\partial \varphi}{\partial Z}, \quad V = -\frac{\partial \varphi}{\partial R} \tag{16}$$

$$\omega = -\frac{\partial^2 \varphi}{\partial Z^2} - \frac{\partial^2 \varphi}{\partial R^2} \tag{17}$$

$$U\frac{\partial \omega}{\partial Z} - V\frac{\partial \omega}{\partial R} = Ra \Pr \frac{\beta_{s_f}}{\beta_{c}} \frac{\partial \theta}{\partial Z} + \frac{\mu_{s_f}}{\rho_{c} \alpha_{c}} \left(\frac{\partial^2 \omega}{\partial Z^2} + \frac{\partial^2 \omega}{\partial Z^2} \right)$$
(18)

$$U\frac{\partial\theta}{\partial Z} - V\frac{\partial\theta}{\partial R} = \frac{\alpha_{sf}}{\alpha_{f}} \left(\frac{\partial^{2}\theta}{\partial Z^{2}} + \frac{\partial^{2}\theta}{\partial Z^{2}} \right)$$
 (19)

where μ is dynamic viscosity, k is thermal conductivity, Ra is Rayleigh number, Gr is Grashof number, Re is Reynolds number, Pr is Prandtl number and Cp is specific heat capacity,

Non-dimensional border conditions are:

$$\begin{split} \Omega \neq &0; \quad \mathbf{V} = \mathbf{0}; \quad \Psi \neq 0; \quad \theta = \mathbf{U} = \mathbf{1} \text{ at } \mathbf{Z} = \mathbf{1}; \ 0 \leq \mathbf{R} \leq \mathbf{1} \ ; \\ U = \Psi = \theta = V = \quad 0 \ ; \ \Omega \neq \ 0 \ ; \quad at \ Z = \ 0; \quad 0 \leq R \leq \mathbf{1} \ ; \\ V = \quad \theta = U = \Psi = \quad 0; \quad \Omega \neq \ 0 \quad at \ R = \ 0; \quad 0 \leq Z \leq \mathbf{1} \ ; \\ \Psi = \quad \frac{\partial U}{\partial \mathbf{R}} = \quad \frac{\partial \theta}{\partial \mathbf{R}} = \quad \frac{\partial V}{\partial \mathbf{R}} = \quad 0; \quad \Omega \neq \mathbf{0} \quad \text{at } \mathbf{R} = \mathbf{1}; \quad 0 \leq Z \leq \mathbf{1} \ . \end{split}$$

The finite difference approach is one of the best problem-solving techniques for nonlinear energy transport and vorticity formulae (18) and (19). The concurrent system of equations was evaluated using relaxation and heat transmission between a fluid and a surface causing a temperature gradient proportional to the neighbouring Nusselt quantity as shown in Eq. (20). [23].

$$Nu_{x} = \frac{h_{x}r}{k} = -\left(\frac{\partial\theta}{\partial Z}\right)_{x} \tag{20}$$

Eq. (20) is the enclosed Nusselt number across the heated contact space yields the usual Nusselt quantity as shown in Eq. (21) [23].

$$N\overline{u} = \frac{\dot{Q}_{conv}}{\dot{Q}_{cond}} = -\int_{0}^{1} \frac{\partial \theta}{\partial Z} \bigg|_{Z=0, rr, 1} dR \tag{21}$$

Equation (22) was used to get the nanofluid's Rayleigh number (Ra_{nf}), Equation (23) was used to calculate its Grashof number (Gr_{nf}), and Equation (24) was used to calculate its Buoyancy factor (BF_{nf}). [11, 23,]

$$Ra_{nf} = \frac{g\beta_{nf}H^3}{\alpha_{nf}\mu_{nf}} \tag{22}$$

$$Gr_{s_i} = \frac{Ra_{s_i}}{Pr_{s_i}} \tag{23}$$

$$BF_{s_i} = \frac{Gr_{s_i}}{\sqrt{\text{Re}}} \tag{24}$$

The condition for stable flow was met by establishing conformity in the temperature and vortex fields as shown in Eq. (25): [3].

$$\frac{\sum_{k=2}^{N} \sum_{j=2}^{M} |\phi_{i}^{n+1} - \phi_{i}^{n}|}{\sum_{k=2}^{N} \sum_{j=2}^{M} |\phi_{i}^{n+1}|} < \delta$$
(25)

The variable ϕ denotes Ω , Ψ or θ , and n refer to the number of iterations required for convergence of the outcomes. The value utilized varies between 10^{-3} and 10^{-8} in distinct forms of literature [3].

III. Results and Discussion

Figure 2 shows the effects of the convergent standard on numerical findings by estimating the average Nusselt value at stability levels from 10^{-1} to 10^{-8} and 10^{-4} convergence worked better. Grid independence experiments demonstrated that a 41 by 41 grid design provided an outstanding numerical solution, high accuracy, and field precision that matched results of [3].

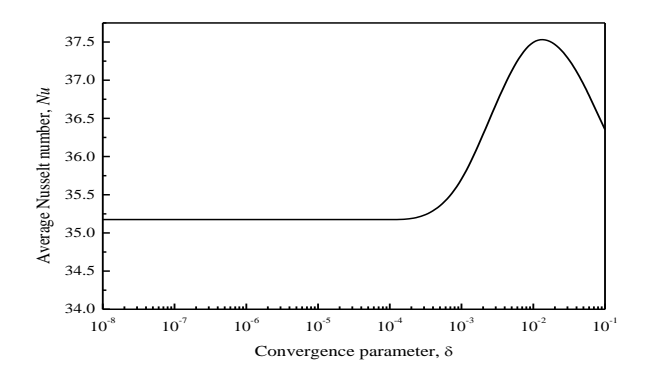


Figure 2: A chart of the convergence parameter against the average Nusselt number

Figure 3 illustrates how changes in the weight proportion of nanoparticles between 0 and 0.1 affect the buoyancy properties of the system.

2.75 x 10³ is the maximum buoyancy value achieved with a weight proportion of 0.04 nanoparticles. It appears that the rate of heat exchange by convection is increasing at a rapid rate, whilst the proportion of nanoparticle volume is decreasing at a rapid rate. As a direct consequence of this, the rate of convective heat transport is fast growing, whilst the change of conduction heat exchange is diminishing.

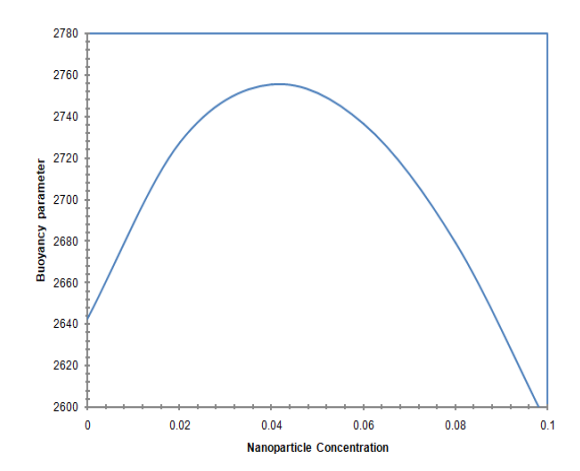


Figure 3: The effect of adjusting the nanoparticle content on the buoyancy variable

The effect that varying the buoyancy variables between 2600 and 2800 has on the Nusselt quantity is seen in Figure 4. The observations made by [19] and [18] are backed up by the values of Nusselt, which rise in conjunction with the buoyancy principles over time. This suggests that while the speed of heat transfer via conduction is decreasing, the rate of heat transmitted by convection is rapidly expanding.

The outcome of changing the buoyancy variables between 2600 and 2800 on the neighborhood drag coefficient is depicted in figure 5. An elevated drag coefficient indicates that the object has greater aerodynamics, while reduced buoyancy values increase aerodynamic drag. Local drag coefficient values are lower in

lockstep with buoyancy attributes, which indicates that convective flow is declining rapidly as buoyancy parameters increase.

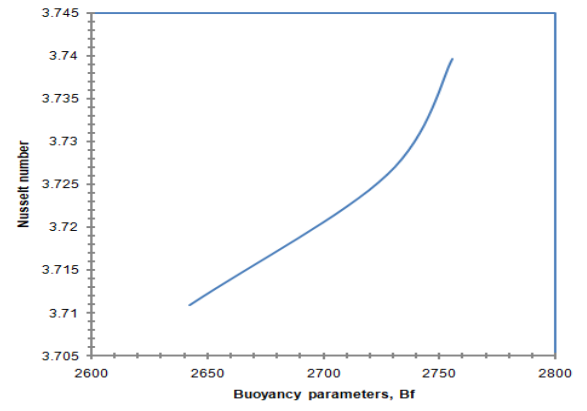


Figure 4: The effect of varied buoyancy characteristics on the Nusselt number.

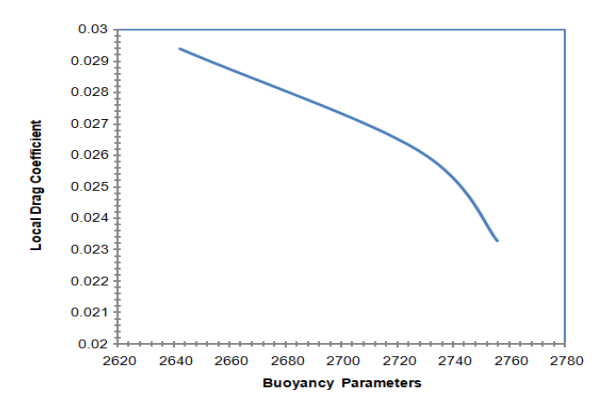


Figure 5: The impact of modifying buoyancy characteristics on the local drag coefficient

Figure 6 illustrates the effect that buoyancy factors have on the temperature of nanofluid when measured along coordinate at a distance of r = 0.5. gradient gets steeper the buoyancy factor gets higher, and the temperature circulation along z gets more uneven from 0 to 0.6 before leveling off at 1 until it reaches 1 and the results were consistent with those obtained by [21].

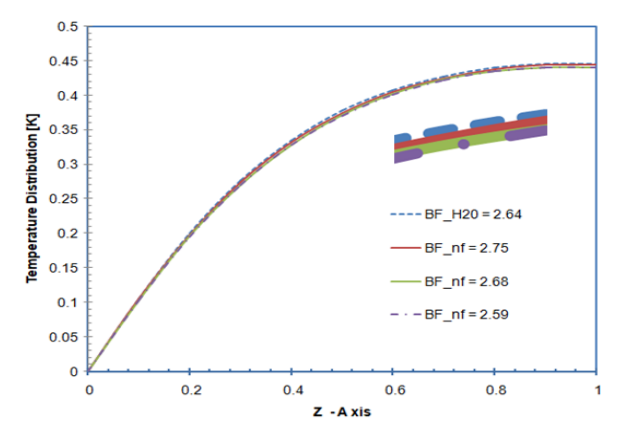


Figure 6: Temperature curve of multiple buoyancy parameters, (Bf*1000) at the midway of the plane

Figure 7 depicts the effect that buoyancy values between 2600 and 2800 have on the longitudinal velocity at the midway of the plane. These values were determined by measuring the velocity of the fluid as it moved along the plane. The longitudinal velocity distribution rises to a higher level as the buoyancy parameters are increased. It suggests that nanofluids with strong buoyancy characteristics create better flow patterns.

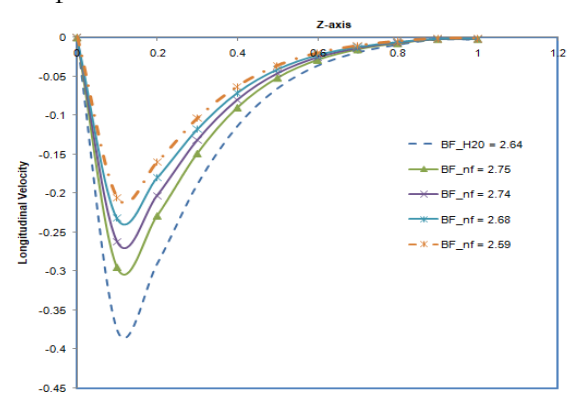


Figure 7: Trajectories of numerous buoyancy parameters (Bf*1000) longitudinal velocities along the Z-axis at the middle plane

The vorticity of a nanofluid is affected by the buoyancy parameter, as seen in Fig. 8. As the buoyancy parameter rises, the nanofluid's vorticity rises. This suggests that nanofluids with higher buoyancy parameters improve flow circulation and rotation patterns. Circulation and vorticity are indicators of fluid rotation, a fluid with a finite surface area rotates in circulations and vorticity makes fluid points rotate.

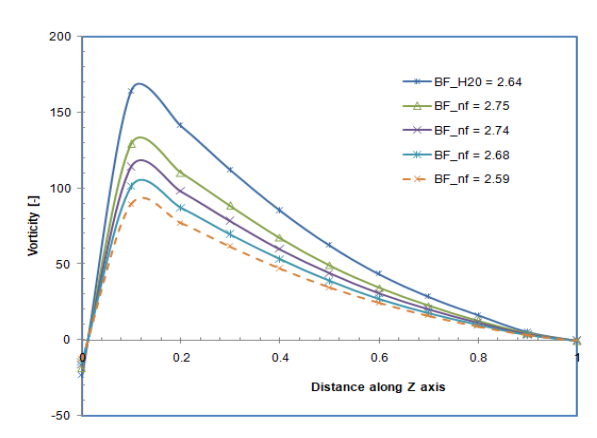


Figure 8: The vorticity patterns for different buoyancy parameters at the center plane of the Z-axis

In Figure 9, the number of buoyancy values is shown versus the stream function. It implies that the stream function of the nanofluid increases when buoyancy parameter values 2600 and 2800 increase, between increasing the volume flow rate of the nanofluids. Engineers examine how floating boats, such as ships and oil rigs, respond to added weight for reasons of safety and efficiency, and this evaluation is based on the density-buoyancy relationship, which is essential in the engineering design of all types of floating vessels. Buoyancy lessens the apparent weight of objects that have completely submerged to the ocean floor and it is frequently simpler to lift an object through water than to take it out of it. It is used for creating ships and submarines.

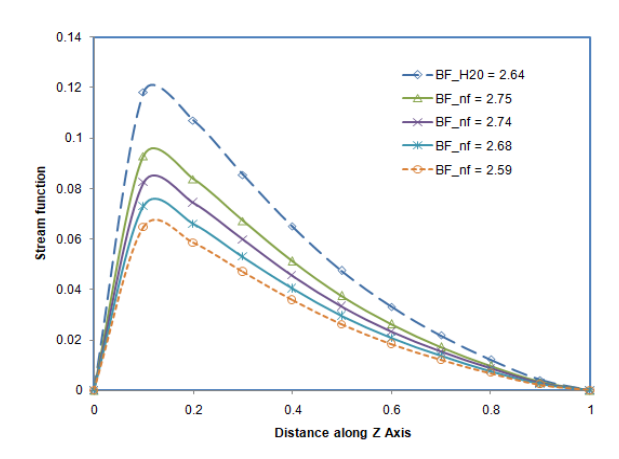


Figure 9: Stream function curves of various Buoyancy parameters, (Bf*1000) along the Z-axis at the midway

IV. Conclusion

This study investigated the effect of buoyancy variables on normal convection in a heated tube filled with Copper (Cu) nanofluid using numerical approaches. The observations led to the following conclusions: the heat dispersion and temperature variation of nanofluids increase as buoyancy parameters increase. When the buoyancy components increase, the stream function, circulation, longitudinal velocity, and rotation increase, while the drag coefficient decreases. This research demonstrates that the effect of a buoyancy parameter modifies both the solution's flow pattern and its thermal behavior. This study contributes to an increased understanding of buoyancy-driven convective flow and heat behavior in the technical design floating vessels to ensure effective performance and safety.

References

[1] Khanafer, K. Vafai, K. and Lightstone, M. "Buoyancy-driven heat transfer enhancement in a two-dimensional enclosure utilizing nanofluids", *International Journal of Heat and Mass Transfer*, vol. 46, no. 19, 2003, pp. 3639-3653

- [2]. Aminossadati, S.M, and Ghasemi, B. "Natural convection cooling of a localized heat source at the bottom of a nanofluid-filled enclosure", *European Journal Mechanical Behaviour Fluids* vol. 28, no. 5, 2009, pp. 630-640
- [3] Sangotayo E. O. and Hunge O. N., "Numerical Analysis of Nanoparticle Concentration Effect on Thermo-physical Properties of Nanofluid in a Square Cavity", International Journal of Mechanical and Production Engineering, vol. 8, no. 2, 2020, pp. 18-23,
- [4] Wen, D. and Ding, Y. "Formulation of nanofluids for natural convective heat transfer applications", *International Journal Heat Fluid Flow*, vol. 26, no. 6, 2005, pp. 855-864
- [5] Nabavitabatabayi, M. Shirani, E. and Rahimian, M.H. "Investigation of heat transfer enhancement in an enclosure filled with nanofluids using multiple relaxation time lattice Boltzmann modeling", *International communication of Heat and Mass Transfer*, vol. 38, 2011, pp. 128-138
- [6] Oztop, H.F. and Abu-Nada, E. "Numerical study of natural convection in partially heated rectangular enclosures filled with nanofluids", *International Journal of Heat and Fluid Flow*, vol. 29, no. 5, 2008, pp. 1326-1336
- [7] Shahi, M. Mahmoudi, A.H. and Talebi, F. "A numerical investigation of conjugated-natural convection heat transfer enhancement of a nanofluid in an annular tube driven by inner heat generating solid cylinder", *International Communication of Heat and Mass Transfer*, vol. 38, no. 4, 2011, pp. 533-542
- [8] Lin, K.C. and Violi, A. "Natural convection heat transfer of nanofluids in a vertical cavity: Effects of nonuniform particle diameter and temperature on thermal conductivity", *International Journal of Heat and Fluid Flow,* vol. 31, 2010, pp. 236-245
- [9] Saleh, H. Roslan, R. and Hashim, I. "Natural convection heat transfer in a nanofluid filled trapezoidal enclosure", *International Journal of Heat and Mass Transfer*, vol. 54, 2011, pp. 194-201
- [10] Nazar, R. Tham, L. Pop, I. and Ingham, D.B. "Mixed convection boundary layer flow from a horizontal circular cylinder embedded in

- a porous medium filled with a nanofluid", *Transport in Porous Media*. vol. 86, no. 2, 2011, pp. 517-536
- [11] Esmaeilpour, M. and Abdollahzadeh, M. "Free convection and entropy generation of nanofluid inside an enclosure with different patterns of vertical wavy walls", *International Journal of Thermal Science*, vol. 52, 2012, pp. 127-136
- [12]. Wen, D., and Ding, Y. "Formulation of Nanofluids for Natural Convective Heat Transfer Applications," *International Journal of Heat Fluid Flow*, vol. 26, no. 6, 2005, pp. 855–864
- [13]. Dongsheng, W., and Yulong, D., 2006, "Natural Convective Heat Transfer of Suspensions of Titanium Dioxide Nanoparticles (Nanofluids)," *IEEE Transactions Nanotechnology*, vol. 5, no. 3, pp. 220–227
- [14]. Prasad, L. S. V., Subrahmanyam, T., Sharma, P. K., Dharmarao, V., and Sharma, K. V., "Turbulent Natural Convection Heat Transfer in Nano-fluids Thermal Stratification—An Experimental Study," *International Journal of Heat and Technology*, vol. 31, 2013, pp. 63–72
- [15]. Rajesh, C., and Sudhakar, S., "Aspect Ratio Dependence of Turbulent Natural Convection in Al₂O₃/ Water Nanofluids," *Applied* Thermal *Engineering*, vol.108, 2016, pp. 1095–1104
- [16]. Hadi, G., Mohsen, S., and Josua, P. M., "Experimental Investigation on Cavity Flow Natural Convection of Al₂O₃ –Water Nanofluids," *International Communications in Heat and Mass Transfer*, vol. 76, 2016, pp. 316–324
- [17]. Seyyadi, S. M., Dayyan, M., Soheil, S., and Ghasemi, "Natural Convection Heat Transfer under Constant Heat Flux Wall in a Nanofluid Filled Annulus Enclosure," *Ain Shams*

- Engineering Journal, vol. 6, no. 1, 2015, pp. 276–280
- [18]. Xiangyin, M., and Yan, L., "Numerical Study of Natural Convection in a Horizontal Cylinder Filled With Water-Based Alumina Nanofluid," *Nanoscale Research Letter*, vol. 10, no. 142, 2015, pp. 1–10
- [19]. Omer, A. A., Nor, A. C. S., and Dawood, H. K., "Natural Convection Heat Transfer in Horizontal Concentric Annulus Between Outer Cylinder and Inner Flat Tube Using Nanofluid," *International Communications in Heat and Mass Transfer*, vol. 57, 2014, pp. 65-71
- [20] Al-Hafidh M.H and Mohammed H.I. "Natural Convection of Nanofluid in Cylindrical Enclosure Filled with Porous Media," *Journal of Energy and Power Engineering*, vol. 7, 2013, pp. 2263-2272
- [21] Rao, S.B. "Buoyancy Induced Natural Convective Heat Transfer in Prismatic Container Filled With Transformer Oil TiO₂ by Vibration Effect on the Cylindrical Surface"; *Journal of Applied Mechanical Engineering*, vol. 10, no. 9, 2021, pp. 1-8
- [22] Sangotayo, E. O and Ogidiga, J. O. "Effect of the Richardson Number on Flow and Heat Transfer in a Cylinder Filled with Cu-Water Nano-fluid at Different Nanoparticle Concentrations," *Journal of Applied Sciences and Environmental Management*, vol. 26, no. 9, 2022, pp.1499-1506
- [23] Waheed, M. A. "Mixed convective heat transfer in rectangular enclosures driven by a continuously moving horizontal plate", *International Journal of Heat and Mass Transfer*, vol. 52, 2009, pp. 5055–5063

NOMENCLATURE

m	Mass flow rate	[kg/hr]
Qu	Useful energy	[W]
C_p	Heat capacity	[J/kg.K]
Cp_{nf}	Nanofluid heat capacity	[J/kg.K]
Cp_f	Fluid heat capacity	[J/kg.K]
Cp_p	Nanoparticle heat capacity	[J/kg.K]
K_f	Fluid thermal conductivity	[W/m.K]
K_p	Nanoparticle thermal conductivity	[W/m.K]
K_{nf}	Nanofluid thermal conductivity	[W/m.K]

Greek Symbols

Symbols	Definitions	Unit
$ ho_{nf}$	Nanofluid density	$[kg/m^3]$
φ	Nanoparticle size	[-]
$ ho_f$	Fluid density	$[kg/m^3]$
μ_{nf}	Nanofluid viscosity	$[m^2/s]$
$ ho_p$	Nanoparticle density	$[kg/m^3]$
μ_f	Fluid viscosity	$[m^2/s]$

Subscripts

nf Nanofluidp Particlef FluidBf Base Fluid

Greek symbols

μ viscosity

 φ Volume fraction

ρ Density